Article

Conservation of μs–ms Enzyme Motions in the Apo- and Substrate-Mimicked State

Heather Beach, Roger Cole, Michelle L. Gill, and J. Patrick Loria

J. Am. Chem. Soc., **2005**, 127 (25), 9167-9176• DOI: 10.1021/ja0514949 • Publication Date (Web): 01 June 2005

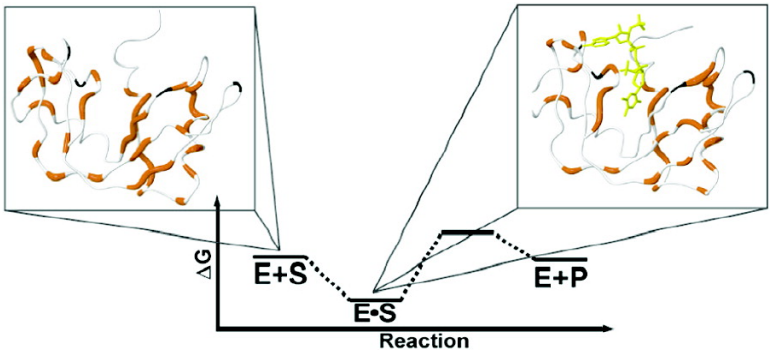

More About This Article

Additional resources and features associated with this article are available within the HTML version:

- Supporting Information
- Links to the 7 articles that cite this article, as of the time of this article download
- Access to high resolution figures
- Links to articles and content related to this article
- Copyright permission to reproduce figures and/or text from this article

View the Full Text HTML

J|A|C|S
ARTICLES
Published on Web 06/01/2005

Conservation of μs−ms Enzyme Motions in the Apo- and Substrate-Mimicked State

Heather Beach,† Roger Cole,† Michelle L. Gill,‡ and J. Patrick Loria*,†

Contribution from the Department of Chemistry and Department of Molecular Biophysics and Biochemistry, Yale University, New Haven, Connecticut 06520

Received March 8, 2005; E-mail: patrick.loria@yale.edu

Abstract: Solution NMR spin-relaxation experiments were used to compare μs−ms dynamics in RNase A in the apo form and as complexed to the substrate-mimic, pTppAp. The crystal structure of the RNase A/pTppAp complex was determined and demonstrates that this ligand binds at the active site and utilizes established substrate binding sites in its interaction with RNase A. Relaxation-compensated CPMG experiments identify flexible residues in and around the active site in both the apo and pTppAp-bound enzyme. Quantitative analysis of the NMR spin-relaxation dispersion curves show that the time scale of motion in RNase A is unchanged when pTppAp binds and is similar to the time scale for the rate-determining step of the catalytic reaction. Temperature-dependent measurements provide an activation barrier for motion of 5.2 $\pm$ 1.0 kcal/mol and 4.5 $\pm$ 1.2 kcal/mol for the apo and pTppAp forms of RNase A, respectively. These data indicate very similar motion exists in the free and bound enzyme. Additionally, chemical shift data suggests that the magnitude of motion is also similar for these two forms and that it is likely that apo enzyme interconverts to a structure that resembles a ligand-bound form. Likewise, it appears that the bound conformation samples the apo enzyme form even when ligand is present. Taken together the data imply that RNase A is in a preexisting dynamic equilibrium between two conformations that represent the open and closed enzyme forms. These data suggest that ligand binding stabilizes the bound conformer but does not induce it.

Introduction

Enzymes undergo conformational fluctuations that span a wide range of time scales. Although it has been established that such motions exist, the role of these motions in the catalytic process is only partially understood. The binding of substrate, substrate analogues, and transition-state analogues often results in conformational changes. This conformational flexibility is essential to the catalytic process as it allows optimal orientation of catalytic residues[1] and provides a suitable environment for the desired reaction.[2] There is also evidence that the inherent flexibility present in enzymes allows sampling of ligand-bound conformations even in the absence of ligand.[3] In these cases, binding serves to stabilize the active conformer, thereby resulting in a population shift toward the active (bound) form. An understanding of this process can be gleaned from a comparison of the kinetics and energetics of enzyme mobility in the apo and ligand-bound states.[4,5] Thus, characterization of protein motion in different ligation states resembling positions along the catalytic reaction coordinate can provide insight into motions that are essential for aspects of catalysis.

Herein we describe the continuation of our efforts to explore the role of flexibility in enzyme function by studying the dynamics of bovine pancreatic ribonuclease A (RNase A). An advantage to the study of RNase A is the availability of data regarding the structure and kinetics of this enzyme. RNase A is a highly stable protein enzyme that catalyzes the cleavage of the P−O$^{5'}$ bond in single-stranded RNA. The active site of the enzyme resides within a deep cleft in the enzyme, and interactions between the enzyme and substrate occur within specific subsites.[6−9] Two subsites, B1 and B2, interact with the nitrogen-containing functional groups of the substrate. The B1 subsite is specific for binding a pyrimidine that is 5′ to the scissile phosphate. Important B1 subsite residues are Thr 45 and Asp 83. The B2 subsite binds the purine base of the nucleotide, 3′ to the cleavage position. This site has a preference for binding adenine, and key residues at this site include Asn 71 and Glu 111. Three phosphate-binding subsites have also been identified in RNase A. The P0 subsite interacts with the 5′ phosphate of the pyrimidine nucleotide and includes Lys 66.

† Department of Chemistry.
‡ Department of Molecular Biophysics and Biochemistry.

(1) Lolis, E.; Petsko, G. A. *Biochemistry* **1990**, *29*, 6619−6625.
(2) Pompliano, D. L.; Peyman, A.; Knowles, J. R. *Biochemistry* **1990**, *29*, 3186−3194.
(3) Williams, J. C.; McDermott, A. E. *Biochemistry* **1995**, *34*, 8309−8319.
(4) Wang, L.; Pang, Y.; Holder, T.; Brender, J. R.; Kurochkin, A. V.; Zuiderweg, E. R. *Proc. Natl. Acad. Sci. U.S.A.* **2001**, *98*, 7684−7689.
(5) Osborne, M. J.; Schnell, J.; Benkovic, S. J.; Dyson, H. J.; Wright, P. E. *Biochemistry* **2001**, *40*, 9846−9859.
(6) Nogues, M. V.; Moussaoui, M.; Boix, E.; Vilanova, M.; Ribo, M.; Cuchillo, C. M. *Cell. Mol. Life Sci.* **1998**, *54*, 766−774.
(7) Pares, X.; Nogues, M. V.; de Llorens, R.; Cuchillo, C. M. *Essays Biochem.* **1991**, *26*, 89−103.
(8) Moussaoui, M.; Nogues, M. V.; Guasch, A.; Barman, T.; Travers, F.; Cuchillo, C. M. *J. Biol. Chem.* **1998**, *273*, 25565−25572.
(9) Fisher, B. M.; Schultz, L. W.; Raines, R. T. *Biochemistry* **1998**, *37*, 17386-17401.

The P1 subsite interacts with the phosphate group containing the scissile bond. In addition to Gln 11, Lys 41, and Asp 121, this site also contains the highly conserved, catalytically critical residues His 12 and His 119. The P2 subsite interacts with the 3′ phosphate of the purine nucleotide and is composed of the residues Lys 7 and Arg 10.

We sought to exploit all of these interactions between enzyme and substrate in an effort to characterize motions present in a complex resembling the first step of an enzyme-catalyzed reaction, namely the enzyme−substrate (E−S) complex. To obtain an effective mimic of the E−S state, the dinucleotide, 5′-phosphothymidine (3′-5′) pyrophosphate adenosine 3′-phosphate (pTppAp),[10] was synthesized to enable the comparison of dynamics present in the free enzyme with the pTppAp/RNase A complex. The molecule pTppAp meets the established criteria for specific base and phosphate binding sites. The use of this molecule allows effective comparisons of the motion present in the apo state and, as described below, the substrate-bound state of the enzyme, and affords an opportunity to characterize motions specific for the enzyme/substrate complex. As part of this study, the structure of pTppAp/RNase A has been determined by X-ray crystallography, the kinetics of binding of pTppAp to RNase A have been measured by NMR line shape analysis, and the internal protein motions have been characterized using NMR spin-relaxation experiments.

Methods and Theory

Protein Expression and Purification. *Escherichia coli* strain BL21-(DE3) was obtained from Novagen (Madison, WI). All buffers and salts were from Aldrich Chemical (St. Louis, MO). Deuterated buffers were from Cambridge Isotope Laboratories (Andover, MA). The plasmid, pBXR, encoding for bovine pancreatic ribonuclease A, was a generous gift of Professor Ronald T. Raines (University of Wisconsin-Madison). ^{15}N isotopically labeled RNase A was expressed and purified according to published protocols, with the exception that the final growth stage was performed in a modified M9 media.[11] The optimized growth media contained 2 g/L ^{15}N NH_4Cl and was supplemented by vitamins and trace metals. The purity of the final samples was determined to be >98% using sodium dodecyl sulfate polyacrylamide gel electrophoresis and mass spectrometry. The concentration of RNase A was assayed spectrophotometrically using an extinction coefficient, $\epsilon_{278} = 9800\ M^{-1}\ cm^{-1}$.[12] The synthesis and characterization of pTppAp was performed as previously reported.[10,13,14]

NMR Experiments. All protein NMR experiments were performed on a 600 μM sample of ^{15}N labeled RNase A. The solution was buffered with 20 mM perdeuterated MES pH 6.3 and contained 10 mM NaCl. NMR data was acquired on a Varian Inova 600 MHz instrument equipped with a Varian HCN probe with triple-axis gradient capabilities, and a Varian Inova 500 MHz spectrometer equipped with a Varian cryogenic HCN probe with *Z*-axis gradients. NMR data were processed with NMRPipe[15] and visualized with Sparky.[16] Relaxation rates were determined as previously described.[17] The NMR sample temperature was calibrated for each experiment with 100% methanol.

Kinetics of pTppAp Binding to RNase A. The interaction of pTppAp with RNase A was studied by NMR line shape analysis. The Bloch−McConnell equations describe the chemical exchange contribution to the NMR line shape.[18] Under steady-state conditions for a case of n chemically exchanging sites:

$$S(\upsilon) = Re\{c\vec{1}(\mathbf{R} - i\Omega - \mathbf{K} - i2\pi\upsilon\mathbf{E})^{-1}\vec{p}\} \quad (1)$$

where S(ν) is the intensity of the spectrum at frequency ν, in Hz.[19] In this notation, c is a normalization factor and $\vec{1}$ is a row vector with all n elements equal to unity. p is a column vector with elements $p_1 \ldots p_n$ in which the elements are the fractional populations of sites 1 to n. The matrix **E** is an unit matrix of dimension n. **R** and Ω are diagonal matrices with elements R_1 to R_n equal to the apparent transverse relaxation rate, R_2^*, and Ω_1 to Ω_n equal to the angular frequencies of the nuclei at each site, respectively. The matrix **K** describes the kinetics of the exchange process. The diagonal elements $K_{r,r}$ are the sum $-\sum_s k_{r,s}$ where $k_{r,s}$ is the rate constant describing the conversion between all sites and site r. The off-diagonal elements of this matrix, $K_{r,s}$ are equal to the first-order rate constant describing the conversion from the r site to the s site.

Although these equations have been derived for unimolecular reactions, they can be applied to the binding of a ligand (L) to an enzyme (E) by considering the process in a unimolecular fashion as illustrated below:

$$E \underset{k_f[L]}{\overset{k_r}{\longleftrightarrow}} EL \quad (2)$$

The dissociation constant for the binding of pTppAp to RNase A has been determined by isothermal titration calorimetry.[13] This dissociation constant allows the calculation of concentrations of ligand (L), free enzyme (E), and ligand-bound enzyme (EL) for each point in the ligand titration. Further, since $K_d = k_r/k_f = 16$ nM,[13] only one of the two rate constants needs to be determined by the fitting process. This reduces the fitting problem to a two-dimensional search for k_r and the normalization factor c.

The kinetics of pTppAp binding to RNase A were measured by titration of pTppAp into a solution of ^{15}N-labeled enzyme. After each titration step, a ^{1}H−^{15}N HSQC spectrum was acquired. The titration was performed at both 25 and 15 °C. The NMR data were initially processed with NMRPipe and then converted with in-house scripts for final analysis with MATLAB (Mathworks, Inc.). A total of 12 peaks were selected that were well-resolved and showed noticeable changes in peak shape and chemical shift during the titration. The two-dimensional peaks were first integrated across the ^{15}N dimension to remove the influence of chemical exchange of the nitrogen atoms on the line shape of the amide proton atoms. The resulting one-dimensional peak shapes for the free enzyme and pTppAp-saturated RNase A were fit to a Lorentzian, after normalization of peak areas, to determine the apparent transverse relaxation rate, R_2^*, and the resonance frequency of the free and bound states. These data were used to construct the **R**, **K**, and Ω matrices and the vector $\vec{p}$. Each of the 10 titration points for all 12 residues were fit simultaneously using a Levenberg−Marquardt algorithm[20] to determine the required normalization factor, c and the rate for substrate dissociation, k_r. Simultaneous fitting is justified because fitting of individual titrations gave similar results (within 10%), suggesting that all report on the same binding process. This overall approach is similar to one recently proposed.[21]

Quantitation of Chemical Exchange. To quantitate the contribution of μs−ms chemical exchange-type motion, the relaxation-compensated CPMG experiment (rcCPMG) was performed as a function of interpulse

(10) Russo, N.; Shapiro, R. *J. Biol. Chem.* **1999**, *274*, 14902−14908.
(11) del Cardayre, S. B.; Ribo, M.; Yokel, E. M.; Quirk, D. J.; Rutter, W. J.; Raines, R. T. *Protein Eng.* **1995**, *8*, 261−273.
(12) Anderson, D. G.; Hammes, G. G.; Walz, F. G., Jr. *Biochemistry* **1968**, *7*, 1637−1645.
(13) Kovrigin, E. L.; Cole, R.; Loria, J. P. *Biochemistry* **2003**, *42*, 5279−5291.
(14) Moffat, J. G.; Khorana, H. G. *J. Am. Chem. Soc.* **1961**, *83*, 663−675.
(15) Delaglio, F.; Grzesiak, S.; Vuister, G.; Zhu, G.; Pfeifer, J.; Bax, A. *J. Biomol. NMR* **1995**, *6*, 277−293.
(16) Goddard, T.; Kneller, D. G. *SPARKY 3*; University of California, San Francisco.
(17) Cole, R.; Loria, J. P. *Biochemistry* **2002**, *41*, 6072−6081.
(18) McConnell, H. M. *J. Chem. Phys.* **1958**, *28*, 430−431.
(19) Reeves, L. W.; Shaw, K. N. *Can. J. Chem.* **1970**, *48*, 3641−3653.
(20) Marquardt, D. W. *J. Soc. Ind. Appl. Math.* **1963**, *11*, 431−441.
(21) Gunther, U. L.; Schaffhausen, B. *J. Biomol. NMR* **2002**, *22*, 201−209.

delay, τ_{cp}.[22] The exchange rate constant k_{ex} for nuclei in equilibrium between two magnetically inequivalent sites (A ↔ B) is the sum of the rate constants for the forward and reverse processes. The value of $R_2(1/\tau_{cp})$ for all time scales is given by [23−25]

$$R_2(1/\tau_{cp}) = \frac{1}{2}\left(R_{2A}^0 + R_{2B}^0 + k_{ex} - \frac{1}{\tau_{cp}}\cosh^{-1}[D_+\cosh(\eta_+) - D_-\cos(\eta_-)]\right) \quad (3)$$

$$D_\pm = \frac{1}{2}\left[\pm 1 + \frac{\Psi + 2\Delta\omega^2}{(\Psi^2 + \zeta^2)^{1/2}}\right] \quad (4)$$

$$\eta_\pm = \frac{\tau_{cp}}{\sqrt{2}}[\pm\Psi + (\Psi^2 + \zeta^2)^{1/2}]^{1/2} \quad (5)$$

$$\Psi = (R_{2A}^0 - R_{2B}^0 - p_A k_{ex} + p_B k_{ex})^2 - \Delta\omega^2 + 4p_A p_B k_{ex}^2 \quad (6)$$

$$\zeta = 2\Delta\omega(R_{2A}^0 - R_{2B}^0 - p_A k_{ex} + p_B k_{ex}) \quad (7)$$

in which p_A and p_B are the equilibrium populations of the two sites, $\Delta\omega$ is the difference in chemical shifts between the two sites, and R_{2A}^0 and R_{2B}^0 are the intrinsic transverse relaxation rates of the two sites in the absence of chemical exchange and k_{ex} is the microscopic exchange rate constant of the motional process. Determination of the microscopic rate constant by measuring R_2 as a function of the inter-pulse delay τ_{cp} is known as dispersion analysis.

Transverse spin-relaxation data using the rcCPMG experiment [22] for the apo and pTppAp-saturated enzyme were acquired at 600 and 500 MHz at 283, 293, and 298 K. At each temperature and static magnetic field, relaxation rates ($R_2(1/\tau_{cp})$) were measured by acquiring two-dimensional experiments with interpulse delays, τ_{cp} in the nitrogen relaxation period of 0.625, 0.714, 1.0, 1.25, 1.67, 2.0, 2.50, 3.33, 5.0, and 10.0 ms. Relaxation rates were measured from a reference experiment with total relaxation time = 0.0 ms and one with the total relaxation time equal to 40.0 ms.[26] The proton carrier frequency was set coincident with the water resonance. The ^{15}N carrier was set to 119 ppm, which is the center of the amide spectral region. Dispersion data for each amino acid residue were analyzed using in-house fitting algorithms written in Mathematica code (Wolfram, Inc) to obtain k_{ex}, $\Delta\omega$, p_a and R_2^0. The fitting protocol utilizes the Levenberg−Marquardt algorithm.[20] Fitting yields the magnitude of $\Delta\omega$ only. To determine the sign of $\Delta\omega$ for the conformational exchange process, HSQC and HMQC experiments were performed at 600 MHz.[27]

Protocol for Dispersion Analysis. Because a large amount of spin-relaxation data was collected for free and bound RNase A at multiple static magnetic field strengths and temperatures, a robust statistical based method was needed to determine which residues were to be analyzed and how that analysis was to be done. This procedure consisted of three steps. (1) The first step involved coarse filtering of the data. At each temperature and magnetic field strength, the residues for which $R_{ex}^* > 3\ s^{-1}$, where $R_{ex}^* = (R_2[\tau_{cp} = 10\ ms] - R_2[\tau_{cp} = 0.625\ ms])$ are chosen for additional analysis. This criterion is based on our experience that R_2 values that differ by 3 s^{-1} over a ~10 ms difference in τ_{cp} represent real differences in relaxation rates, thereby indicating the presence of conformational exchange motion for this residue. The goal at this stage is to pare down the data sets to a manageable size and identify only residues involved in μs−ms motion. (2) To quantitate the motional parameters, χ^2 analysis of the fits of eq 3 to the individual dispersion data is performed. Residues with χ^2 values greater than that defined by the $\alpha = 0.05$ critical value are not considered for further analysis. At this stage, all residues undergoing conformational exchange motion have been identified from step 1, and a subset of these, from step 2, with suitable data quality in their dispersion curves for more detailed analysis has been found. (3) In typical proteins that show exchange motion, there are often several residues experiencing that motion. Therefore, it is of interest to ask whether each residue experiences independent motion or is part of a global motional process in which motional parameters k_{ex} and p_a are shared among residues unlike $\Delta\omega$ and R_2^0, which are residue specific parameters. To differentiate between a global process and residue-specific motion, the relaxation−dispersion data is fit by eq 3 in which k_{ex} and p_a are overall fit parameters with a single value and $\Delta\omega$ and R_2^0 are individual, residue-specific fit parameters. Fitting is done using in-house written Perl scripts that generate the Mathematica notebook, which performs the data analysis. The results of this fitting procedure are compared to one in which all four parameters are allowed residue-specific values. The Akaike Information Criterion (AIC) is then used to assess which model (global k_{ex}, p_a or individual values) is more likely to describe the data.[28] In addition, a runs test analysis of the fit residuals is performed to ensure no systematic trend is present. This test checks that the residuals reflect a random distribution at the 95% confidence level.

X-ray Crystallography. The pTppAp/RNase A complex was crystallized by the hanging drop vapor diffusion method using PEG-4000 as a precipitant. The protein−ligand complex was taken from an NMR sample, which contained 600 μM ^{15}N-labeled RNase A and 20% molar excess of pTppAp, the same used for NMR relaxation experiments. The sample also contained 10% D_2O, 10 mM NaCl, 3mM NaN_3 and 20 mM MES-d_{13} at pH 6.3. Within one week rod clusters of pTppAp-bound RNase A crystals appeared above solutions containing between 33.5% (w/v) and 38% (w/v) PEG-4000. These rodlike crystals were used to seed crystals suitable for X-ray analysis, which had a final PEG concentration of 29%. The X-ray diffraction data was acquired on a Nonius Kappa CCD diffractometer system operating with graphite monochromated Mo Kα radiation at a wavelength of 0.71069 Å. The resulting data were processed with DENZO and SCALEPACK.[29] The scaled data were provided as input to the program Crystallography and NMR System (CNS), which was employed for the structure calculation.[30] All visualization of enzyme structure and electron density maps was performed with the program O.[31]

Results

Structure of RNase A/pTppAp. X-ray diffraction data indicated a primitive monoclinic cell with parameters $a = 31.09$ Å, $b = 75.84$ Å, $c = 51.82$ Å, $\alpha = \gamma = 90°$, $\beta = 106.35°$ that belonged to the $P2_1$ space group. Two datasets were ultimately collected. The first data set collected contained 10267 unique reflections extending to 2.3 Å. A second, larger data set was collected that contained 14927 unique reflections extending to 2.0 Å. These two data sets were merged. Two RNase A molecules were identified in the asymmetric unit. Overall the polypeptide chain fit well to the electron density, particularly in the first protomer. The second protomer showed three short surface regions where the electron density was rather low,

(22) Loria, J. P.; Rance, M.; Palmer, A. G. *J. Am. Chem. Soc.* **1999**, *121*, 2331−2332.
(23) Carver, J. P.; Richards, R. E. *J. Magn. Reson.* **1972**, *6*, 89−105.
(24) Davis, D. G.; Perlman, M. E.; London, R. E. *J. Magn. Reson., Ser. B* **1994**, *104*, 266−275.
(25) Jen, J. *J. Magn. Reson.* **1978**, *30*, 111−128.
(26) Mulder, F. A.; Skrynnikov, N. R.; Hon, B.; Dahlquist, F. W.; Kay, L. E. *J. Am. Chem. Soc.* **2001**, *123*, 967−975.
(27) Skrynnikov, N. R.; Dahlquist, F. W.; Kay, L. E. *J. Am. Chem. Soc.* **2002**, *124*, 12352−12360.
(28) Akaike, H. In *Information theory and an extension of maximum likelihood principles*, Proceedings of the 2nd international symposium on information theory, Budapest, 1973; Petrov, B. N., Csaki, F., Eds.; Budapest, 1973; pp 267−281.
(29) Otwinowski, Z.; Minor, W. *International Tables for Crystallography*; Kluwer: New York, 1997; F.
(30) Brunger, A. T.; Adams, P. D.; Clore, G. M.; DeLano, W. L.; Gros, P.; Grosse-Kunstleve, R. W.; Jiang, J. S.; Kuszewski, J.; Nilges, M.; Pannu, N. S.; Read, R. J.; Rice, L. M.; Simonson, T.; Warren, G. L. *Acta Crystallogr., Sect. D* **1998**, *54*, 905−921.
(31) Jones, T. A.; Zou, J. Y.; Cowan, S. W.; Kjeldgaard, M. *Acta Crystallogr., Sect. A* **1991**, *47* (Pt 2), 110−119.

Table 1. Refinement Statistics for the X-ray Data from the pTppAp/RNase A Complex

Crystal Parameters		
space group	$P2_1$ (two molecules per asymmetric unit)	
unit cell parameters	$a = 31.09$ Å $b = 75.84$ Å $c = 51.82$ Å $\alpha = \gamma = 90°$ $\beta = 106.35°$	
Data Statistics		
wavelength	0.71069 Å	0.71069Å
resolution	19.6−2.3 Å	19.6−2.0 Å
number of reflections measured	28381	51556
number of unique reflections	10257	14927
completeness (outermost shell)	99.0% (98.0%)	99.9% (99.8%)
R_{symm}	7.4%	7.8%
Merged Data Set		
total number of unique reflections		15654
completeness		99.9%
R_{merge}		9.2%
$I/\sigma I$		16.1
Refinement Statistics		
resolution		19.6 Å − 2.0 Å
number of reflections used ($\|F\| > 0$)		14950
R_{cryst}		21.9%
R_{free}		25.9%
Model Statistics		
number of protein atoms		1902
number of ligand atoms		102
number of solvent molecules		77
Deviations for Ideality (rms)		
bond lengths		0.0058 Å
bond angles		1.2°
dihedral angles		23.17°
impropers		0.7°
Average B Factor (Å^2) (Molecule I/Molecule II)		
main chain atoms		19.6/31.9
side chain atoms		23.5/33.9
all protein atoms		25.8/28.1
ligand atoms		27.7/ 27.7
solvent atoms		29.5

primarily in the loop regions around Ser 22, Arg 39, and Lys 91. These regions have higher average *B* factors for the second molecule main-chain and side-chain atoms. These same regions are well resolved in the first protomer. The RNase A/pTppAp structure was solved using the method of molecular replacement. The molecular replacement model was built from the Protein Databank file 1QHC, which contains the coordinates for the RNase A/5′-phosphodeoxyuridine (3′-5′) pyrophosphate adenosine 3′-phosphate (pdUppAp).[32] The two protomers of RNase A/pTppAp in the asymmetric unit are related by pure translational noncrystallographic symmetry. After the initial molecular replacement, each protomer was refined independently. The final structure had a resolution of 2.0 Å with $R_{free} = 25.9\%$. A summary of refinement statistics is presented in Table 1. The coordinates have been deposited in the RCSB protein data bank[33] under the accession number 1U1B.

A comparison of the peptide backbone structures between apo RNase A and the RNase A/pTppAp complex shows small differences (Figure 1a). The backbone RMSD between these two enzyme forms is 0.69 Å, and the RMSD for all atoms is 1.26 Å. The areas where the backbone conformations are noticeably different are the loop regions near Ser 22 and Lys 91 as well as the region near Asn 67 and Lys 66. The β-sheet near Asn 67 has moved slightly toward the pTppAp molecule. Stereo figures highlighting the differences in the enzyme structure between the free and bound forms are provided in the Supporting Information. The pTppAp molecule is present in the active site of both protomers in the asymmetric unit. The conformation of the ligand is identical between both molecules of RNase A, and all atoms are well resolved in the electron density map, as seen in Figure 1b. The conformation of the adenosine nucleotide glycosyl torsion angle is syn. The glycosyl torsion angle of the thymidine portion of the ligand is anti. The conformation of the sugar rings for both the adenosine and thymidine portion of pTppAp bound to RNase A is *C2′-endo*.

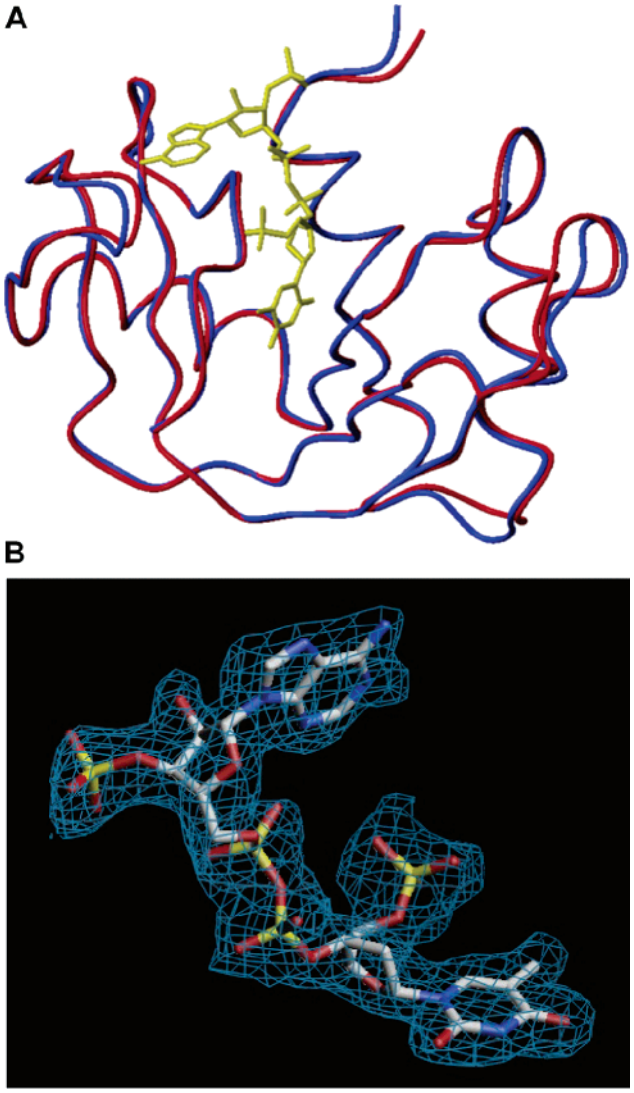

Figure 1. Crystal structures of RNase A. In (A) ribbon representation of an overlay of apo RNase A (blue) and RNase A/pTppAp (red) PDB code 1U1B. Shown in yellow is pTppAp bound to the active site of RNase A. In (B) a stick diagram of pTppAp in the configuration it assumes when bound to RNase A, superimposed on the $(2F_o - F_c)$ electron density contoured at 1.1σ. The crystal structure for apo RNase A is from 7RSA.[34] (A) is generated with the program MolMol.[35]

(32) Leonidas, D. D.; Shapiro, R.; Irons, L. I.; Russo, N.; Acharya, K. R. *Biochemistry* **1999**, *38*, 10287−10297.
(33) Berman, H. M.; Westbrook, J.; Feng, Z.; Gilliland, G. L.; Bhat, T. N.; Weissig, H.; Shindyalov, I. N.; Bourne, P. E. *Nucleic Acids Res* **2000**, *28*, 235−242.

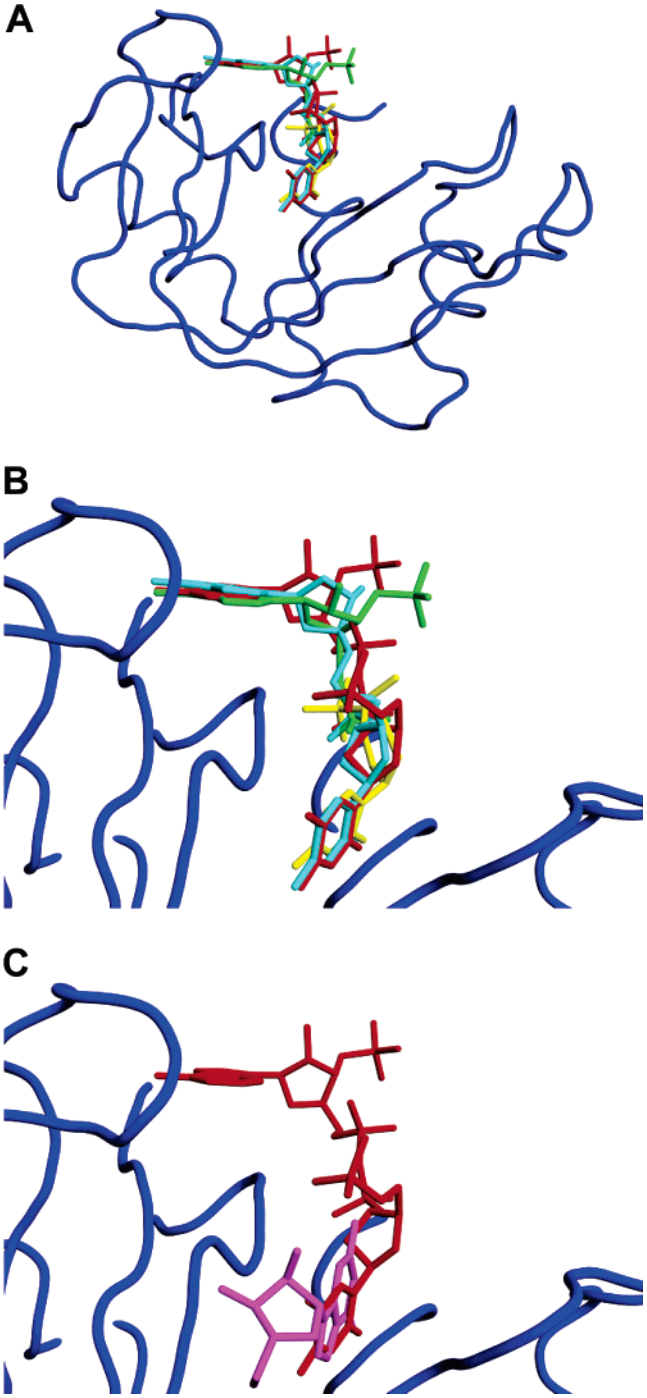

Figure 2. Comparison of ligand structures. (A) Overlay of the X-ray structures of the bound pTppAp (red), with product analogues 3′-CMP (yellow)[37] and pAp (green),[36] and substrate analogue, dCpA (cyan).[37] The structure of RNase A/pTppAp determined in this work is shown as a blue ribbon. In (B) a close-up of the active site from (A) is shown. In (C) the same view as in (B) shows a comparison of the conformations of pTppAp (red) and the nonproductively bound uridyl (2′-5′) guanosine (magenta) with only the guanosine portion visible.[43] The structure of RNase A/pTppAp determined in this work is shown as a blue ribbon. The crystal structures of all enzyme complexes were superimposed along the amino acid backbone; only the backbone of RNase A bound to pTppAp is shown. The figure was prepared with the program PyMOL (DeLano Scientific, 2002).

Torsion angles β and γ for both the adenosine and thymidine bases are $-ac$ and $+sc$, respectively. These data indicate a very similar overall conformation between pTppAp and pdUppAp (not shown). Shown in Figure 2 are overlays of the RNase A/pTppAp structure with substrate analogue dCpA, and product-state analogues 3′-CMP and pAp. Figure 2c shows a comparison of the bound pTppAp conformation with that of the guanosine portion of the nonproductively bound cytosine (2′-5′) guanosine.

pTppAp binds in the active site of RNase A and is in close contact with functionally important residues. The adenine portion binds in the B2 subsite. The purine base forms an aromatic stack above the imidazole ring of His 119 with the exocyclic amino nitrogen (N6) of adenosine within hydrogen bonding distance with the side chains of Asn 67, Gln 69, and Asn 71. These interactions are similar to those observed with pAp.[36] The 3′-phosphate of the adenine group sits in the P2 subsite with Oγ1 4.0 Å from Nζ of Lys 7. In addition, the side chain Nδ1 atom of His 119 is 3.2 Å from the oxygen that it would protonate as part of the transphosphorylation reaction if pTppAp were a reactive substrate. The catalytic base for the transphosphorylation reaction, His 12, is located near the ribose C2; however, because C2 is deoxy, no reaction occurs with pTppAp. It appears that the majority of interactions expected in the true RNase A/substrate complex are realized in the pTppAp complex, and this complex is distinct from unproductively bound ligands (Figure 2c).

Kinetics of pTppAp Binding to RNase A. In previous studies, titration calorimetry was used to characterize the thermodynamics of pTppAp binding to RNaseA.[13] Here, line shape fitting of RNase A resonances from a pTppAp titration series was used to characterize ligand binding kinetics. These experiments were performed at 288 and 298 K. The results of these titrations are shown in Figure 3. Fitting each residue to the same set of kinetics parameters provided a good fit in all cases. Fitting to more complex models (e.g., three-site) did not improve the quality of the fits. Fitted parameters are presented in Table 2. Assuming Arrhenius behavior, the activation barrier for ligand release determined from data at these two temperatures is 16.5 ± 1.2 kcal/mol and that for ligand binding is 4.3 ± 3.8 kcal/mol.

NMR Spin-Relaxation Experiments. At each temperature, residues in RNase A and RNase A/pTppAp exhibited evidence of conformational exchange broadening as indicated by increases in measured R_2 values as τ_{cp} increases. Based on typical signal-to-noise values in our experiments, R_{ex} [R_2(10 ms) − R_2(0.625 ms)] values > 3 s^{-1} are considered significant and indicative of μs−ms motion. Using this criterion, apo RNase A contains 25, 43, and 29 residues in conformational exchange at 283, 293, and 298 K, respectively, at 500 and 600 MHz combined. Flexible residues in the apo form agree well with those identified previously;[17] the use of two magnetic fields[39] in this work allowed a more thorough characterization of the exchange parameters. For the RNase A/pTppAp complex at both magnetic field strengths, the number of exchanging residues is 36, 36, and 23 at 283, 293, and 298 K respectively. These flexible residues are mapped onto the RNase A structure in Figure 4.

(34) Wlodawer, A.; Svensson, L. A.; Sjolin, L.; Gilliland, G. L. *Biochemistry* **1988**, *27*, 2705−2717.
(35) Koradi, R.; Billeter, M.; Wuthrich, K. *J. Mol. Graph.* **1996**, *14*, 51−55, 29−32.
(36) Leonidas, D. D.; Chavali, G. B.; Oikonomakos, N. G.; Chrysina, E. D.; Kosmopoulou, M. N.; Vlassi, M.; Frankling, C.; Acharya, K. R. *Protein Sci.* **2003**, *12*, 2559−2574.
(37) Zegers, I.; Maes, D.; Dao-Thi, M. H.; Poortmans, F.; Palmer, R.; Wyns, L. *Protein Sci.* **1994**, *3*, 2322−2339.
(38) Leonidas, D. D.; Shapiro, R.; Irons, L. I.; Russo, N.; Acharya, K. R. *Biochemistry* **1997**, *36*, 5578−5588.
(39) Millet, O. M.; Loria, J. P.; Kroenke, C. D.; Pons, M.; Palmer, A. G. *J. Am. Chem. Soc.* **2000**, *122*, 2867−2877.

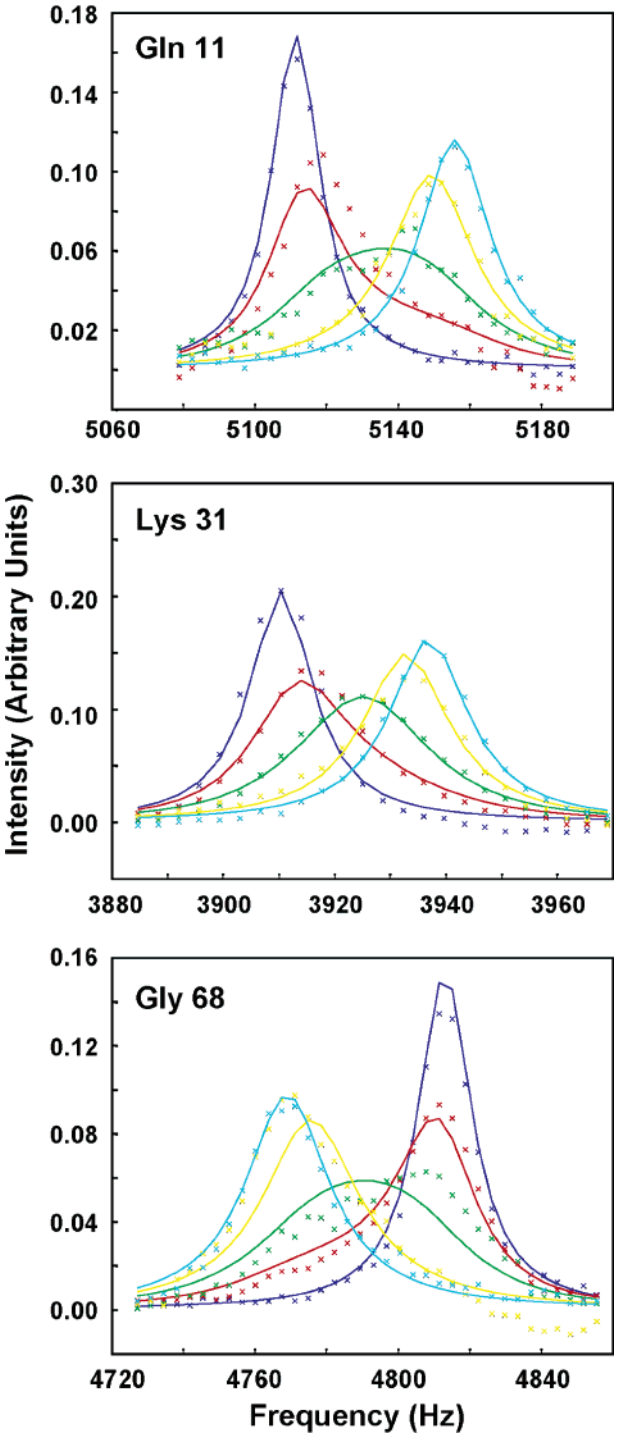

Figure 3. Line shape fitting results for the pTppAp titration. Titration data is shown for residues Gln 11, Lys 31, and Gly 68. Experimental data points are shown in the same color as the fitted line obtained using best fits with eq 1. The curves represent the proton chemical shift dependence and peak intensity at 0.0, 0.3, 0.6, 0.9, 1.2 (blue, red, green, yellow, cyan) equivalents of pTppAp; although the titration consisted of 10 points, only these five are shown for clarity.

In favorable cases, the NMR data were of sufficient quality to allow quantitation of the exchange parameters by fitting eq 3 to the spin-relaxation data (see Methods and Theory). For the apo form at 500 and 600 MHz, seven residues (S16, T17, S22, D83, T100, Q101, and H119) at 283 K, thirteen residues (Q11, S15, S16, T17, N44, F46, A64, K66, N71, D83, T100, Q101, and H119) at 293 K, and nine residues (S16, T17, S22, N44, K66, N71, D83, T100, and Q101) at 298 K were globally fit to eq 3. In the RNase A/pTppAp complex, the number of residues at each temperature that were fit to eq 3 were 12 (F8, E9, S15, A19, S22, N34, K41, S80, C84, E86, A96, and A122) at 283 K; 10 (Q11, S15, S16, T17, A19, K66, G68, T70, Q101, A122) at 293 K; and 8 (Q11, M13, S16, T17, S22, M30, Q101, and H119) at 298 K. The protocol described in the Methods and Theory was used to determine that a global model in which all residues have the same k_{ex} value and equilibrium site populations is appropriate for RNase A in the apo and pTppAp case. In all cases, a conformational exchange model in which k_{ex} and p_a are global parameters was a better representation of the data than one in which all parameters can assume a residue specific value as determined by comparison of AIC results (Supporting Information). Simultaneous fitting of eq 3 to the spin-relaxation data at both magnetic fields yielded exchange rate constants, k_{ex}, of 1080 ± 80 s^{-1} {930−1240 95% CI} at 283 K, 1390 ± 70 s^{-1} {1240−1540} at 293 K, and 1750 ± 130 s^{-1} {1490−2020} at 298 K for apo RNase A and 1316 ± 160 s^{-1} {990−1640}, 1880 ± 200 s^{-1} {1490−2272}, and 1920 ± 250 s^{-1} {1410−2420} for the RNase A/pTppAp complex at 283, 293, and 298 K respectively. Examples of dispersion curves are shown in Figure 5.

Table 2. Results of pTppAp Titration Lineshape Analysis

temperature (K)	k_f ($M^{-1}s^{-1}$)	k_r (s^{-1})	K_d (nM)
288	$3.9 \pm 0.8 \times 10^9$	30 ± 5	8 ± 1
298	$4.9 \pm 0.6 \times 10^9$	80 ± 5	16 ± 2

The exchange rate of the conformational motion process increases with increasing temperature. The value of k_{ex} versus temperature is plotted in Figure 6 for the apo and pTppAp forms of RNase A. The variation of $\ln(k_{ex})$ vs T^{-1} was fit with the Arrhenius equation, yielding activation energies for the motional process of 5.2 ± 1.0 and 4.5 ± 1.2 kcal/mol for the apo and pTppAp forms, respectively. In contrast to the temperature dependence of k_{ex} there is little overall variation in equilibrium populations with temperature. For the apo form the population of the major conformation ranges from 90 to 93% over the 15° temperature range, whereas in the pTppAp form the population ranges from 90 to 96%. However, in neither case is a discernible trend observed in the temperature dependence of the population. This most likely reflects the uncertainty in fitting for p_a in addition to the fact that the populations may simply have a weak dependence on temperature.

Fitting spin-relaxation data with eq 3 also provides the magnitude of the chemical shift difference ($\Delta\omega$) between exchanging sites. There are eight residues (Q11, S15, S16, T17, S22, K66, Q101, H119) that have quantifiable $\Delta\omega$ values from the global fits of the dispersion data for both forms of RNase A. Figure 7 shows the correlation of $\Delta\omega$ values for the apo and pTppAp forms. The correlation coefficient (R^2) is 0.47 if Lys 66 and His 119 are included in the fit and 0.94 and a slope of 0.96 without inclusion of these residues.

Discussion

Many enzymes catalyze reactions that greatly favor formation of product with little or no reverse reaction, and RNase A is included in this group. This irreversibility precludes NMR study of enzyme dynamics during the catalytic cycle for all but a few

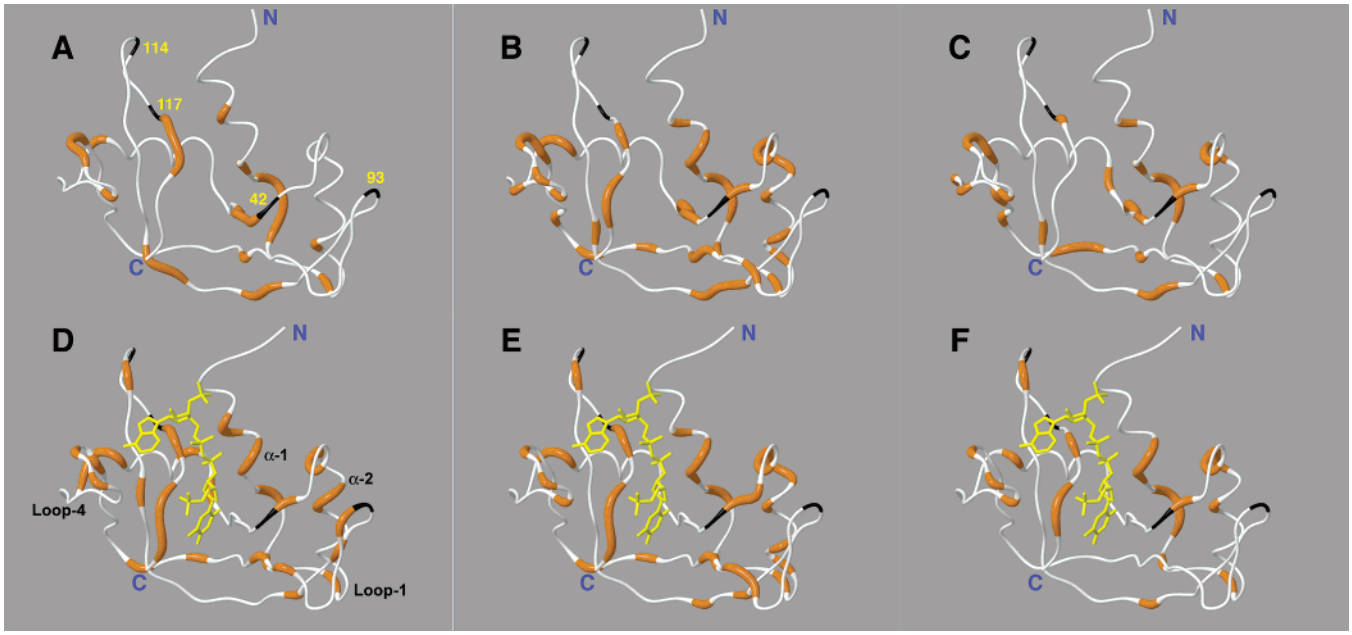

Figure 4. Location of conformationally flexible residues. Amino acid residues with $R_{ex} > 3\ s^{-1}$ are mapped onto the structure as the larger diameter orange ribbon. In panels A, B, and C exchanging residues in the apo form are shown at 283, 293, and 298 K, respectively. Panels D, E, and F show the flexible residues in the pTppAp complex at 283, 293, and 298 K, respectively. The pTppAp molecule is shown in yellow. The N- and C termini are identified. Proline residues are numbered and shown in black in (A) and selected 2° structure elements indicated in (D) to help orient the reader.

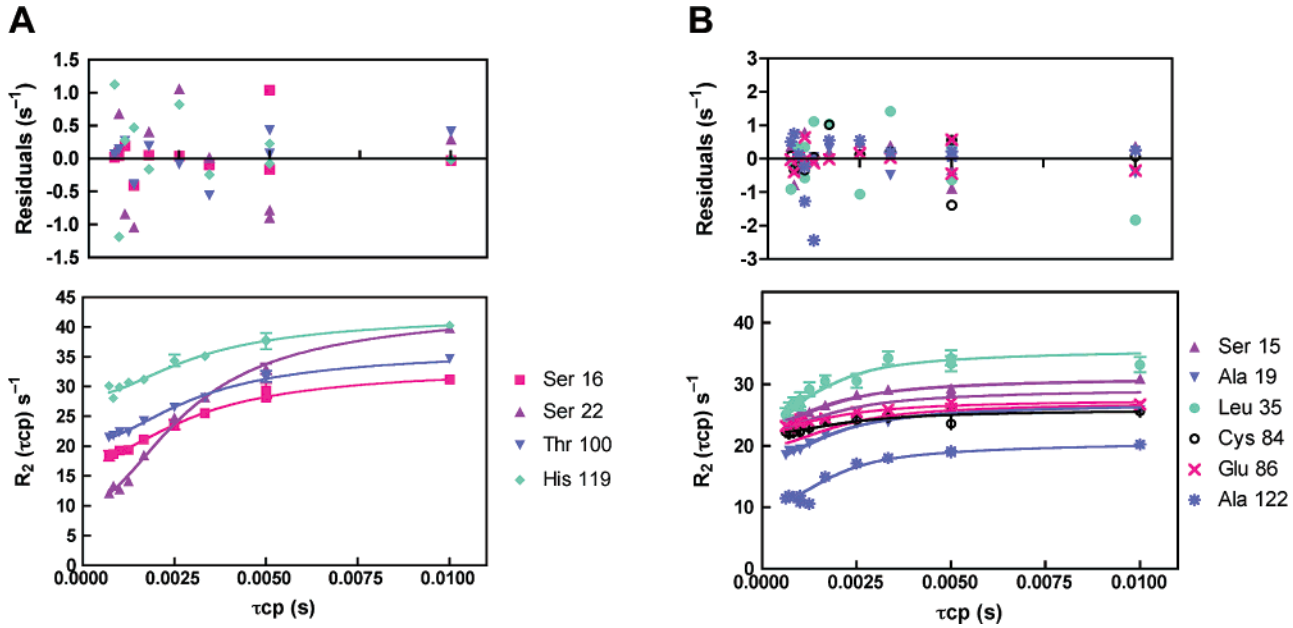

Figure 5. ^{15}N relaxation dispersion data for RNase A. Dispersion curves for apo (A) and pTppAp bound (B) RNase A at 283 K and 600 MHz. Curves represent a global fit of eq 3 to the relaxation data. Fit residuals are shown above each graph. Runs analysis shows no significant trend in the residuals. Error bars on the individual data points are determined from duplicate experiments.

cases.[40] A general alternative is to use unreactive small molecules that bind to the enzyme to mimic various stages along the reaction coordinate. This technique has long been used to address mechanistic issues.[41,42] Here, we employ this approach to study enzyme dynamics in a substrate-like state using the tight-binding dinucleotide, pTppAp.

To verify that pTppAp interacts with RNase A in a manner similar to that predicted for the actual substrate, we solved the X-ray crystal structure of RNase A/pTppAp to 2.0 Å resolution. Analysis of the resulting structure indicates that indeed the ligand makes all major contacts with RNase A previously identified for substrate-like molecules (Figures 1 and 2). The purine and pyrimidine moieties of pTppAp bind in the correct base subsites, while the phosphate groups interact with the appropriate amino acids in the P0, P1, and P2 subsites. It is also evident from Figure 2b,c that the conformation of pTppAp is similar to those of substrate and product-like molecules and distinct from that of molecules that bind unproductively.[43] Therefore motions detected in the RNase A/pTppAp complex

(40) Eisenmesser, E. Z.; Bosco, D. A.; Akke, M.; Kern, D. *Science* **2002**, *295*, 1520−1523.
(41) Wolfenden, R. *Nature* **1969**, *223*, 704−705.
(42) Radzicka, A.; Wolfenden, R. *Biochemistry* **1991**, *30*, 4160−4164.

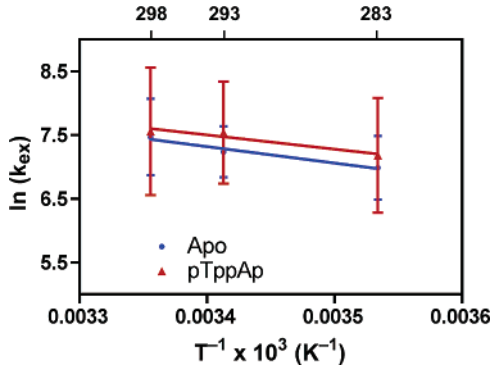

Figure 6. Temperature dependence of k_{ex}. An Arrhenius plot of ln k_{ex} with $1/T$ for apo (blue) and pTppAp (red) RNase A. At the top of the graph the temperature in Kelvin is shown.

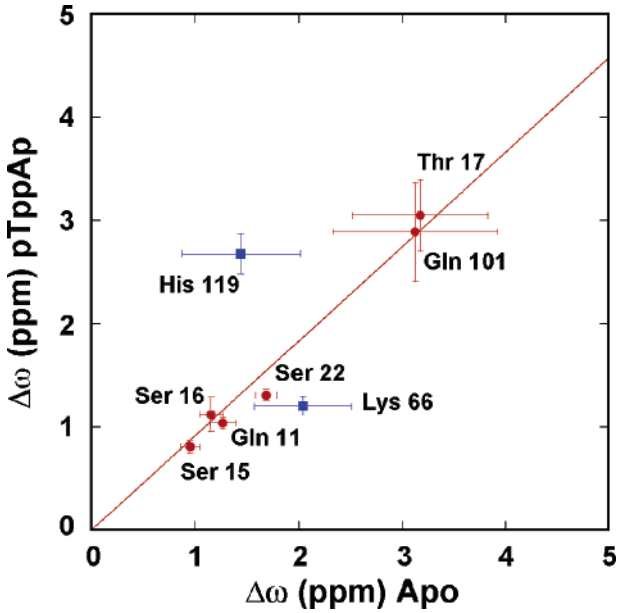

Figure 7. Chemical shift differences in RNase A complexes. Correlation of $\Delta\omega$ values determined by global fitting with eq 3 for residues with quantifiable data in both the apo and pTppAp forms of RNase A. The red line represents a linear fit to the data points for Q11, S15, S16, T17, S22, and Q101. Data for H119 and K66, shown in red, are excluded from this fit.

are expected to reflect those occurring when RNase A interacts with substrate. Furthermore, comparison of these motions with motions in the apo enzyme will reveal dynamic processes important for function and those unique to each form of the enzyme. The changes in conformation between the free and pTppAp forms are subtle, yet comparison of X-ray structures of free and ligand-bound RNase A suggests these changes are real and linked to ligand binding. The conformational change is summarized by a reduction in the size of the active-site groove upon binding. The active site is situated between two halves of the enzyme that open and close, thereby changing the shape of the groove. The bottom of the active site plays a role as the hinge in this motion.[44] These structural changes that occur upon binding are localized to the loop-1 (residues 14−24) that connects α-helix-1 and α-helix-2. This loop is located at the bottom of the active-site pocket. The other region that experiences a change in conformation upon ligand binding is loop-4 (residues 64−71), which comprises the B2 subsite.

The regions in RNase A that exhibit different free and bound conformations are also the regions of the enzyme that undergo conformational motion, as evidenced by dynamic NMR data. This motion appears to be necessary for optimal binding/release of ligands, which can be understood as follows. RNase A becomes more compact upon binding as the enzyme "tightens" its grip on the ligand.[45] Interestingly, the rate-limiting step for RNase A catalysis is not chemical but is instead the product release step.[46,47] Several studies have characterized the kinetics of product release in RNase A under solution conditions similar to those used in the current NMR experiments. At 298 K, the off-rate for 3′-CMP is 3×10^3 s^{-1} measured by T-jump experiments,[48] and 2×10^3 s^{-1} for 3′-UMP using ^{31}P NMR.[49] As stated in other work, the product release step is likely linked to the opening/closing of the active site, which occurs at a rate $\sim 10^3$ s^{-1}.[50] As would be expected for rate-limiting product release, the value of k_{cat} is the same as that for product dissociation. For the catalytic transphosphorylation of UpA k_{cat} is reported to be 1400−2900 s^{-1} at pH = 6.0.[11,51] These values match the conformational exchange rate measured here for the free and pTppAp-bound RNase A. It is worth noting that this NMR-observed motion is intramolecular in nature, i.e., not stemming from direct binding or release. This is established by our line shape analysis from pTppAp titrations, which indicates that binding/dissociation of the pTppAp molecule does not contribute to the measured exchange phenomena. In addition, under the equilibrium conditions of the NMR experiments only 0.02% of RNase A is not complexed to pTppAp. Therefore, binding and release dynamics negligibly contribute to the observed relaxation dispersion, indicating that our analysis informs on intramolecular motions only. Thus, we conclude that because pTppAp is a confirmed substrate mimic, this argument safely extends to natural substrates. RNase A/pTppAp conserves the intramolecular motion and inherent flexibility of free RNase A. Furthermore, the time scale of this conserved motion matches the rate-limiting product release step. The activation energy for the conformational change in RNase A and RNase A/pTppAp are identical within the uncertainty of the measurement. The activation barrier for this conformational change is similar to that observed for the product dissociation step of 3′-UMP (E_{act} = 3.5 kcal/mol).[49] These data suggest that RNase A possesses a natural motion of interconversion between two conformations on a time scale of the rate-determining enzymatic step, likely to facilitate product release. The similarity in k_{ex} and E_{act} for the two forms of RNase A suggests a similarity in the type of motion that is occurring. An important remaining question concerns the molecular basis for this motion.

A qualitative estimate of the structural alterations as a result of molecular motion can be determined from differences, $\Delta\omega$, in chemical shift between open and closed conformations. We

(43) Aguilar, C. F.; Thomas, P. J.; Moss, D. S.; Mills, A.; Palmer, R. A. *Biochim. Biophys. Acta* **1991**, *118*, 6−20.
(44) Hammes, G. G. *Biochemistry* **2002**, *41*, 8221−8228.
(45) Dubins, D. N.; Filfil, R.; Macgregor, R. B.; Chalikian, T. V. *J. Phys. Chem. B* **2000**, *104*, 390−401.
(46) Thompson, J. E.; Venegas, F. D.; Raines, R. T. *Biochemistry* **1994**, *33*, 7408−7414.
(47) Park, C.; Raines, R. T. *Biochemistry* **2003**, *42*, 3509−3518.
(48) Cathou, R. E.; Hammes, G. G. *J. Am. Chem. Soc.* **1965**, *86*, 3240−3245.
(49) Lee, G. C.; Chan, S. I. *Biochem. Biophys. Res. Commun.* **1971**, *43*, 142−148.
(50) Hammes, G. G. *Enzyme Catalysis and Regulation*; Academic Press: New York, 1982.
(51) Witzel, H.; Barnard, E. A. *Biochem. Biophys. Res. Commun.* **1962**, *7*, 295−299.

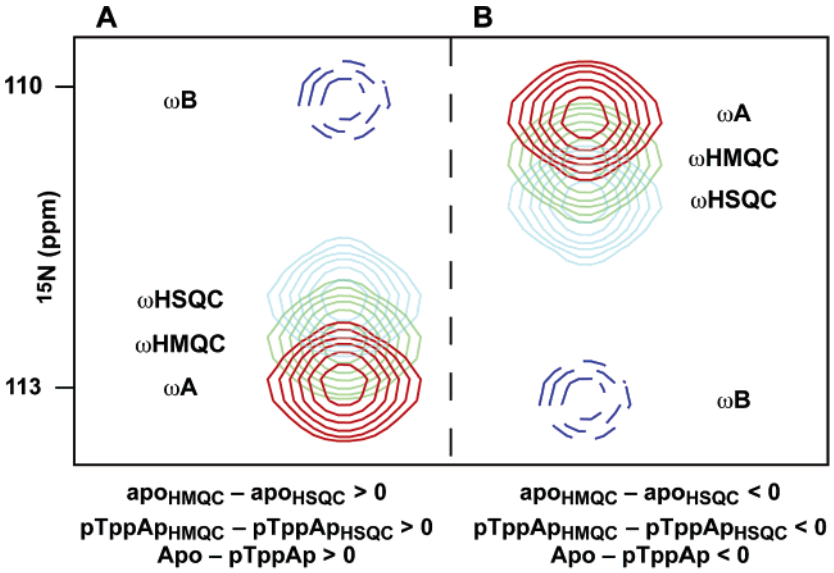

C

Residue	(±) Δω (Apo – pTppAp)	(±) Δω (apo-HMQC – apo-HSQC)	(±) Δω (pTppAp-HMQC – pTppAp-HSQC)
Q11	+	+	–
M13	–	+	–
S15	–	–	+
S16	–	–	+
T17	+	+	–
S22	–	–	+
M30	+	+	+
L35	–	–	–
K41	+	+	–
C58	–	–	+
K66	+	+	–
G68	+	+	–
T70	–	–	–
S80	+	+	+
T99	+	+	+
Q101	–	–	+
V118	+	+	+
H119	+	+	–
D121	–	+	–
A122	+	–	+

Figure 8. Determination of the sign of $\Delta\omega$. The sign of $\Delta\omega$ can be determined as shown in (A, B) as described.[27] The two scenarios that give rise to positive (A) and negative (B) sign of $\Delta\omega$. The intrinsic resonance position, in the absence of conformational exchange, is shown for the major conformer (red) at ω_A and the minor (blue dashed) conformer at ω_B. In the presence of conformational exchange, the observed resonance in an HSQC experiment is closer to that of the minor, invisible resonance than that of the HMQC peak. Therefore, if the resonance of the major conformer is downfield from that of the minor conformer, the sign of $\Delta\omega$ is positive (for $\omega_{HMQC} - \omega_{HSQC}$). If the resonance of the major conformer is upfield from that for the minor resonance, then the sign of $\Delta\omega$ is negative (for $\omega_{HMQC} - \omega_{HSQC}$). In (C) the sign of $\Delta\omega$ for residues in conformational exchange was determined from HMQC and HSQC experiments and is shown in the third and fourth columns of (C). The second column shows the sign of the chemical shift difference, $\Delta\omega_{bind}$, between the apo and pTppAp resonances (for $\omega_{Apo} - \omega_{pTppAp}$) for the same residues. If, as suggested in this work, the apo enzyme explores the bound conformation, then the signs of columns 2 and 3 would be expected to be the same and that of column 4 should be opposite those of 2 and 3. This is exactly what is observed for the majority of residues with the exception of those highlighted.

determined $\Delta\omega$ for residues that show exchange in both the apo and the pTppAp RNase A forms (Figure 7). There is an excellent linear correlation, with a slope = 0.96, between the magnitude of $\Delta\omega$ for apo and RNase A/pTppAp; the appropriate sign variation of $\Delta\omega$ has been demonstrated separately (vide infra). This suggests that the two conformations of the interconverting species are similar for the free and bound forms of RNase A. That is, the apo form samples the bound conformation, and likewise the RNase A/pTppAp complex samples the free enzyme conformation (although pTppAp does not dissociate from the enzyme). Several of these residues are located in loop-1 that undergoes a significant conformational change upon ligand binding. These residues are located at the bottom of the active site near the hinge region. An exception to the noted correlation in chemical shift changes is observed for His 119 and Lys 66, both of which are in close proximity to a phosphate group of the bound pTppAp molecule. It is likely that the phosphate perturbs the chemical shift of these residues significantly so that the calculated $\Delta\omega$ value in the bound form incorporates an additional Coulombic effect not at play in the free enzyme.[4]

The sign of $\Delta\omega$ was determined from two-dimensional HMQC and HSQC spectra (Figure 8).[27] The intramolecular conformational motion that our data support as intrinsic to both the apo and substrate-bound forms of RNase A further suggests that ligand binding shifts a thermodynamic equilibrium between open and closed conformations. This notion is supported by our comparison of the signs of ^{15}N chemical-shift changes $\Delta\omega_{conf}$ and $\Delta\omega_{bind}$. The sign of the shift change from binding is self-evident in the progression of NMR peaks through a series of ligand-titration spectra. For example, the sign of $\Delta\omega_{bind}$ is given by the difference in peak positions in the HSQC for apo and HSQC for pTppAp-bound RNase A, as shown in column 2 of Figure 8c. The sign of $\Delta\omega_{conf}$ is more subtly obtained according to the observation by Kay and co-workers that HSQC spectra exhibit exchange-averaged peaks closer to the minor conformer's "invisible" resonance than do the corresponding peaks in HMQC spectra.[27] Figure 8 illustrates this effect. To substantiate the idea that binding induces a population shift in a conserved, intrinsic opened/closed dynamic, we compared the signs of $\Delta\omega_{conf}$(apo) and $\Delta\omega_{bind}$ for 20 residues that both exhibit the exchange dynamic and shift significantly upon binding pTppAp: Q11, M13, S15, S16, T17, S22, M30, L35, K41, C58, K66, G68, T70, S80, T99, Q101, V118, H119, D121, A122. Seventeen of these have the same sign for $\Delta\omega_{bind}$ (apo − pTppAp; column 2) and for $\Delta\omega_{conf}$ (apo-HMQC − apo-HSQC; column 3), as shown in Figure 8c. This result is expected for an apo enzyme that includes a minor conformer resembling the bound form. Considering the pTppAp-bound enzyme (Figure 8c), we find that $\Delta\omega_{bind}$ (apo − pTppAp; column 2) carries the opposite sign of $\Delta\omega_{conf}$ (bound-HMQC − bound-HSQC; column 4) for 14 of the noted 20 residues. This conversely indicates that the bound enzyme includes a minor conformation similar to the average apo structure.

The data presented here indicate that RNase A possesses flexibility in and around the active site and that this motion is conserved when binding the substrate analogue pTppAp. The identical exchange rates and activation barriers for free and bound forms imply that the motion in both cases is similar. In addition, the occurrence of this motion on the same time scale as the rate-limiting product release step suggests that motion observed by NMR and the motion that controls the overall catalytic rate are the same. Chemical shift data support a scenario where RNase A samples the apo and bound conformations regardless of the presence of ligand. The binding of a molecule at the active site simply shifts the equilibrium toward the bound conformer. Overall, it appears that amino acid residues that line the bottom of the active site as well as loop residues in the substrate-binding site act in concert with catalytically essential residues to modulate motion in RNase A that is required for product release.

Finally, it is likely that small differences exist in the structures of the bound conformer sampled in the absence of ligand and the bound conformation measured in the presence of ligand. Much of the substrate binding specificity originates from the sidechain residues in RNase A and the conformations of these sidechains may be different in RNase A when it is bound to different nucleotides thereby indicating the existence of several different bound conformations. Thus, the subtleties of the bound conformation, in particular at the sidechain positions may very well exhibit variability even though the studies in this work suggest the gross features of protein backbone exist in equilibrium between two conformations.

The preservation of μs−ms motion upon binding ligand, as described in this study, presents an additional view of protein dynamics when compared with other work from our lab that demonstrated rigidification of RNase A dynamics on the ps−ns time scale upon interaction with pTppAp.[13] These studies suggest that consideration of these dynamical effects could aid in the design of more potent enzyme inhibitors.

Acknowledgment. We thank Dr. Chris Incarvito (Yale) for help with the X-ray crystallography and Dr. James Kempf (Yale) for critical comments on the manuscript. We thank Prof. Jeff Peng (University of Notre Dame) for productive discussions regarding these studies at the 2005 ENC. M.L.G and R.C. are supported by NSF graduate research fellowships. H.B. acknowledges support from an NIH Biophysical Training Grant. J.P.L. acknowledges support from an NSF CAREER Grant (MCB-0236966). J.P.L. is an Alfred P. Sloan Fellow.

Supporting Information Available: Table containing AIC results from dispersion analysis and two stereo figures comparing apo and bound RNase A structures. This material is available free of charge via the Internet at http://pubs.acs.org.

JA0514949

Table S1. AIC Results from Global vs Individual fitting

Temperature (K)	Apo		pTppAp	
	Global AIC	Indiv. AIC	Global AIC	Indiv. AIC
283	92.2	102.5	92.1	171.0
293	165.8	282.9	227.6	301.0
298	115.2	144.3	147.7	179.4

Figure S1.

A

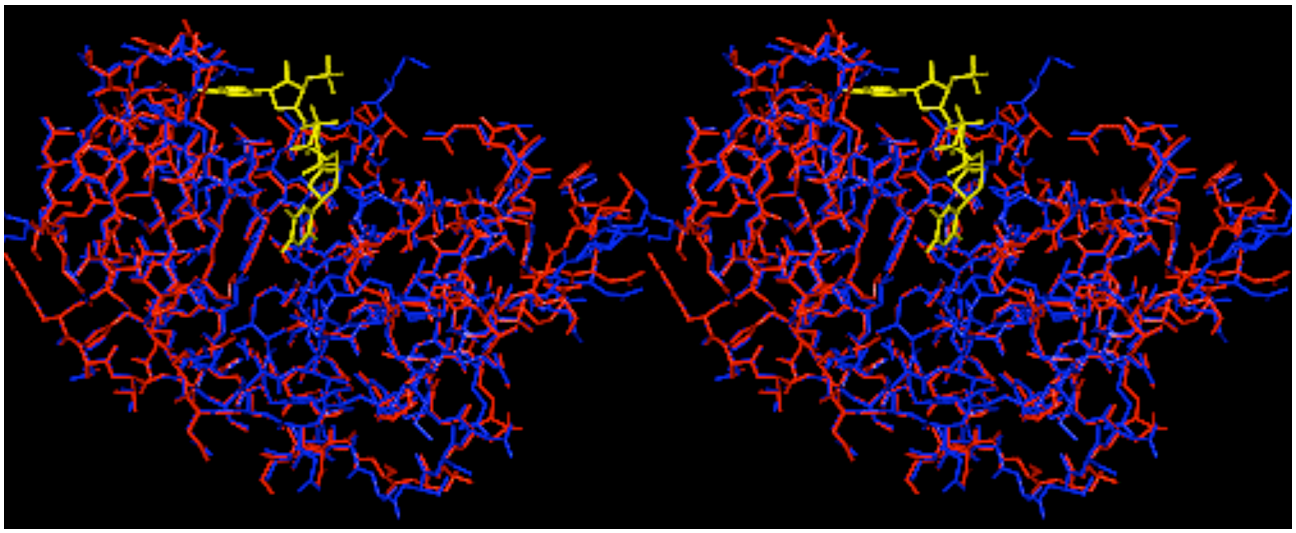

B

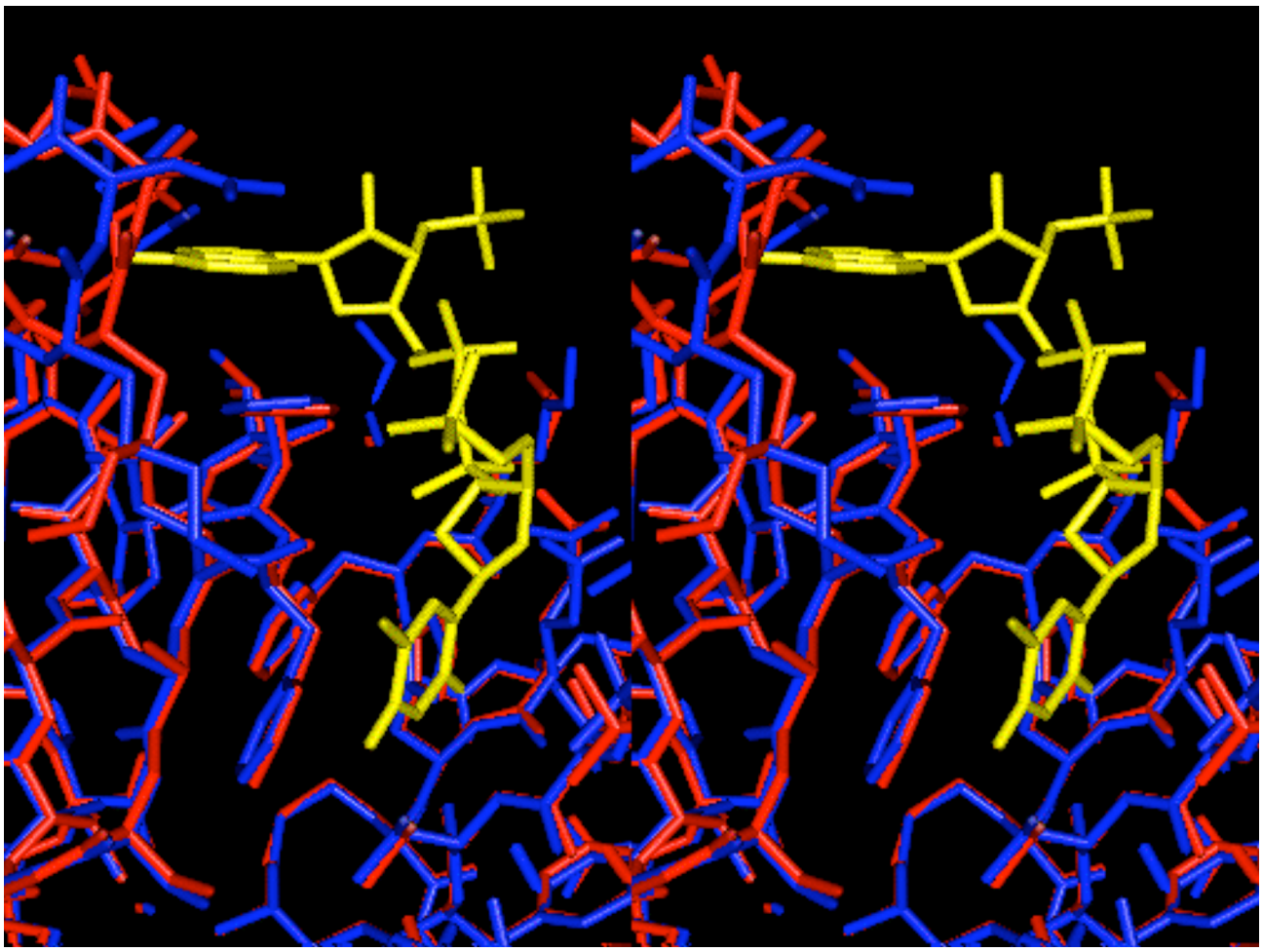

Figure S1. Stereo view of the crystal structures of RNase A. In (A) ribbon representation of an overlay of apo RNase A (blue) and RNase A/pTppAp (red) PDB code 1U1B. Shown in yellow is pTppAp bound to the active site of RNase A. In (B) a closeup of the active site is shown in identical color scheme as (A). The crystal structure for apo RNase A is from 7RSA.[1] (A) generated with the program MolMol.[2]

References:

1 Wlodawer, A.; Svensson, L. A.; Sjolin, L.; Gilliland, G. L., *Biochemistry* 1988, 27, 2705-2717.

2 Koradi, R.; Billeter, M.; Wuthrich, K., *J Mol Graph* 1996, 14, 51-5, 29-32.